EUROPEAN ORGANIZATION FOR NUCLEAR RESEARCH

CERN–PPE/96-75

7 June 1996

Search for the lightest chargino at $\sqrt{s} = 130$ and 136 GeV

DELPHI Collaboration

Abstract

A search for pair production of the lightest chargino at $\sqrt{s}$ = 130.4 and 136.3 GeV has been carried out using the data sample corresponding to the 5.92 pb^{-1} recorded by the DELPHI detector during the high energy run of LEP in the last period of 1995. The theoretical reference model has been the Minimal Supersymmetric Standard Model with R-parity conservation. The three topologies expected for the decay of a pair of charginos, namely two acoplanar leptons plus missing energy ($\ell\ell$), two jets and an isolated lepton plus missing energy ($jj\ell$) and missing energy in a hadronic environment ($4j$), were investigated. No evidence of a signal was found. Lower mass limits were derived for various scenarios, including the case of a low mass difference between the chargino and the neutralino and of a light sneutrino. The mass limits range between 56.3 GeV/c^2 and the kinematic limit.

(Submitted to Physics Letters B)

P.Abreu[21], W.Adam[50], T.Adye[37], E.Agasi[31], I.Ajinenko[42], R.Aleksan[39], G.D.Alekseev[16], R.Alemany[49], P.P.Allport[22], S.Almehed[24], U.Amaldi[9], S.Amato[47], A.Andreazza[28], M.L.Andrieux[14], P.Antilogus[9], W-D.Apel[17], Y.Arnoud[39], B.Åsman[44], J-E.Augustin[25], A.Augustinus[9], P.Baillon[9], P.Bambade[19], F.Barao[21], R.Barate[14], M.Barbi[47], D.Y.Bardin[16], A.Baroncelli[40], O.Barring[24], J.A.Barrio[26], W.Bartl[50], M.J.Bates[37], M.Battaglia[15], M.Baubillier[23], J.Baudot[39], K-H.Becks[52], M.Begalli[6], P.Beilliere[8], Yu.Belokopytov[9,53], K.Belous[42], A.C.Benvenuti[5], M.Berggren[47], D.Bertini[25], D.Bertrand[2], F.Bianchi[45], M.Bigi[45], M.S.Bilenky[16], P.Billoir[23], D.Bloch[10], M.Blume[52], T.Bolognese[39], M.Bonesini[28], W.Bonivento[28], P.S.L.Booth[22], C.Bosio[40], O.Botner[48], E.Boudinov[31], B.Bouquet[19], C.Bourdarios[9], T.J.V.Bowcock[22], M.Bozzo[13], P.Branchini[40], K.D.Brand[36], T.Brenke[52], R.A.Brenner[15], C.Bricman[2], R.C.A.Brown[9], P.Bruckman[18], J-M.Brunet[8], L.Bugge[33], T.Buran[33], T.Burgsmueller[52], P.Buschmann[52], A.Buys[9], S.Cabrera[49], M.Caccia[28], M.Calvi[28], A.J.Camacho Rozas[41], T.Camporesi[9], V.Canale[38], M.Canepa[13], K.Cankocak[44], F.Cao[2], F.Carena[9], L.Carroll[22], C.Caso[13], M.V.Castillo Gimenez[49], A.Cattai[9], F.R.Cavallo[5], V.Chabaud[9], M.Chapkin[42], Ph.Charpentier[9], L.Chaussard[25], P.Checchia[36], G.A.Chelkov[16], M.Chen[2], R.Chierici[45], P.Chliapnikov[42], P.Chochula[7], V.Chorowicz[9], V.Cindro[43], P.Collins[9], J.L.Contreras[19], R.Contri[13], E.Cortina[49], G.Cosme[19], F.Cossutti[46], H.B.Crawley[1], D.Crennell[37], G.Crosetti[13], J.Cuevas Maestro[34], S.Czellar[15], E.Dahl-Jensen[29], J.Dahm[52], B.Dalmagne[19], M.Dam[29], G.Damgaard[29], P.D.Dauncey[37], M.Davenport[9], W.Da Silva[23], C.Defoix[8], A.Deghorain[2], G.Della Ricca[46], P.Delpierre[27], N.Demaria[35], A.De Angelis[9], W.De Boer[17], S.De Brabandere[2], C.De Clercq[2], C.De La Vaissiere[23], B.De Lotto[46], A.De Min[36], L.De Paula[47], C.De Saint-Jean[39], H.Dijkstra[9], L.Di Ciaccio[38], F.Djama[10], J.Dolbeau[8], M.Donszelmann[9], K.Doroba[51], M.Dracos[10], J.Drees[52], K.-A.Drees[52], M.Dris[32], J-D.Durand[25], D.Edsall[1], R.Ehret[17], G.Eigen[4], T.Ekelof[48], G.Ekspong[44], M.Elsing[52], J-P.Engel[10], B.Erzen[43], M.Espirito Santo[21], E.Falk[24], D.Fassouliotis[32], M.Feindt[9], A.Ferrer[49], S.Fichet[23], T.A.Filippas[32], A.Firestone[1], P.-A.Fischer[10], H.Foeth[9], E.Fokitis[32], F.Fontanelli[13], F.Formenti[9], B.Franek[37], P.Frenkiel[8], D.C.Fries[17], A.G.Frodesen[4], R.Fruhwirth[50], F.Fulda-Quenzer[19], J.Fuster[49], A.Galloni[22], D.Gamba[45], M.Gandelman[6], C.Garcia[49], J.Garcia[41], C.Gaspar[9], U.Gasparini[36], Ph.Gavillet[9], E.N.Gazis[32], D.Gele[10], J-P.Gerber[10], M.Gibbs[22], R.Gokieli[51], B.Golob[43], G.Gopal[37], L.Gorn[1], M.Gorski[51], Yu.Gouz[45,53], V.Gracco[13], E.Graziani[40], G.Grosdidier[19], K.Grzelak[51], S.Gumenyuk[28,53], P.Gunnarsson[44], M.Gunther[48], J.Guy[37], F.Hahn[9], S.Hahn[52], Z.Hajduk[18], A.Hallgren[48], K.Hamacher[52], W.Hao[31], F.J.Harris[35], V.Hedberg[24], R.Henriques[21], J.J.Hernandez[49], P.Herquet[2], H.Herr[9], T.L.Hessing[35], E.Higon[49], H.J.Hilke[9], T.S.Hill[1], S-O.Holmgren[44], P.J.Holt[35], D.Holthuizen[31], S.Hoorelbeke[2], M.Houlden[22], J.Hrubec[50], K.Huet[2], K.Hultqvist[44], J.N.Jackson[22], R.Jacobsson[44], P.Jalocha[18], R.Janik[7], Ch.Jarlskog[24], G.Jarlskog[24], P.Jarry[39], B.Jean-Marie[19], E.K.Johansson[44], L.Jonsson[24], P.Jonsson[24], C.Joram[9], P.Juillot[10], M.Kaiser[17], F.Kapusta[23], K.Karafasoulis[11], M.Karlsson[44], E.Karvelas[11], S.Katsanevas[3], E.C.Katsoufis[32], R.Keranen[4], Yu.Khokhlov[42], B.A.Khomenko[16], N.N.Khovanski[16], B.King[22], N.J.Kjaer[29], H.Klein[9], A.Klovning[4], P.Kluit[31], B.Koene[31], P.Kokkinias[11], M.Koratzinos[9], K.Korcyl[18], V.Kostioukhine[42], C.Kourkoumelis[3], O.Kouznetsov[13,16], P.-H.Kramer[52], M.Krammer[50], C.Kreuter[17], I.Kronkvist[24], Z.Krumstein[16], W.Krupinski[18], P.Kubinec[7], W.Kucewicz[18], K.Kurvinen[15], C.Lacasta[49], I.Laktineh[25], J.W.Lamsa[1], L.Lanceri[46], D.W.Lane[1], P.Langefeld[52], V.Lapin[42], I.Last[22], J-P.Laugier[39], R.Lauhakangas[15], G.Leder[50], F.Ledroit[14], V.Lefebure[2], C.K.Legan[1], R.Leitner[30], Y.Lemoigne[39], J.Lemonne[2], G.Lenzen[52], V.Lepeltier[19], T.Lesiak[18], J.Libby[35], R.Lindner[52], A.Lipniacka[36], I.Lippi[36], B.Loerstad[24], J.G.Loken[35], J.M.Lopez[41], D.Loukas[11], P.Lutz[39], L.Lyons[35], J.MacNaughton[50], G.Maehlum[17], A.Maio[21], T.G.M.Malmgren[44], V.Malychev[16], F.Mandl[50], J.Marco[41], R.Marco[41], B.Marechal[47], M.Margoni[36], J-C.Marin[9], C.Mariotti[40], A.Markou[11], T.Maron[52], C.Martinez-Rivero[41], F.Martinez-Vidal[49], S.Marti i Garcia[49], F.Matorras[41], C.Matteuzzi[9], G.Matthiae[38], M.Mazzucato[36], M.Mc Cubbin[9], R.Mc Kay[1], R.Mc Nulty[22], J.Medbo[48], M.Merk[31], C.Meroni[28], S.Meyer[17], W.T.Meyer[1], M.Michelotto[36], E.Migliore[45], L.Mirabito[25], W.A.Mitaroff[50], U.Mjoernmark[24], T.Moa[44], R.Moeller[29], K.Moenig[9], M.R.Monge[13], P.Morettini[13], H.Mueller[17], L.M.Mundim[6], W.J.Murray[37], B.Muryn[18], G.Myatt[35], F.Naraghi[14], F.L.Navarria[5], S.Navas[49], K.Nawrocki[51], P.Negri[28], S.Nemecek[12], W.Neumann[52], N.Neumeister[50], R.Nicolaidou[3], B.S.Nielsen[29], M.Nieuwenhuizen[31], V.Nikolaenko[10], P.Niss[44], A.Nomerotski[36], A.Normand[35], M.Novak[12], W.Oberschulte-Beckmann[17], V.Obraztsov[42], A.G.Olshevski[16], A.Onofre[21], R.Orava[15], K.Osterberg[15], A.Ouraou[39], P.Paganini[19], M.Paganoni[9,28], P.Pages[10], R.Pain[23], H.Palka[18], Th.D.Papadopoulou[32], K.Papageorgiou[11], L.Pape[9], C.Parkes[35], F.Parodi[13], A.Passeri[40], M.Pegoraro[36], L.Peralta[21], H.Pernegger[50], M.Pernicka[50], A.Perrotta[5], C.Petridou[46], A.Petrolini[13], M.Petrovyck[28,53], H.T.Phillips[37], G.Piana[13], F.Pierre[39], M.Pimenta[21], S.Plaszczynski[19], O.Podobrin[17], M.E.Pol[6], G.Polok[18], P.Poropat[46], V.Pozdniakov[16], M.Prest[46], P.Privitera[38], N.Pukhaeva[16], A.Pullia[28], D.Radojicic[35], S.Ragazzi[28], H.Rahmani[32], J.Rames[12], P.N.Ratoff[20], A.L.Read[33], M.Reale[52], P.Rebecchi[19], N.G.Redaelli[28], M.Regler[50], D.Reid[9], P.B.Renton[35], L.K.Resvanis[3], F.Richard[19], J.Richardson[22], J.Ridky[12], G.Rinaudo[45], I.Ripp[39], A.Romero[45], I.Roncagliolo[13], P.Ronchese[36], L.Roos[14], E.I.Rosenberg[1], E.Rosso[9], P.Roudeau[19], T.Rovelli[5], W.Ruckstuhl[31], V.Ruhlmann-Kleider[39], A.Ruiz[41], K.Rybicki[18], H.Saarikko[15], Y.Sacquin[39], A.Sadovsky[16], O.Sahr[14], G.Sajot[14], J.Salt[49], J.Sanchez[26], M.Sannino[13], M.Schimmelpfennig[17], H.Schneider[17], U.Schwickerath[17], M.A.E.Schyns[52], G.Sciolla[45], F.Scuri[46], P.Seager[20], Y.Sedykh[16], A.M.Segar[35], A.Seitz[17], R.Sekulin[37], L.Serbelloni[38], R.C.Shellard[6], I.Siccama[31], P.Siegrist[39], S.Simonetti[39], F.Simonetto[36], A.N.Sisakian[16], B.Sitar[7], T.B.Skaali[33], G.Smadja[25], N.Smirnov[42], O.Smirnova[24], G.R.Smith[37], R.Sosnowski[51], D.Souza-Santos[6], T.Spassov[21], E.Spiriti[40], P.Sponholz[52], S.Squarcia[13], C.Stanescu[40], S.Stapnes[33], I.Stavitski[36], K.Stevenson[35], F.Stichelbaut[9], A.Stocchi[19], J.Strauss[50], R.Strub[10], B.Stugu[4], M.Szczekowski[51], M.Szeptycka[51], T.Tabarelli[28], J.P.Tavernet[23], E.Tcherniaev[42],

O.Tchikilev[42], J.Thomas[35], A.Tilquin[27], J.Timmermans[31], L.G.Tkatchev[16], T.Todorov[10], S.Todorova[10], D.Z.Toet[31], A.Tomaradze[2], A.Tonazzo[28], L.Tortora[40], G.Transtromer[24], D.Treille[9], W.Trischuk[9], G.Tristram[8], A.Trombini[19], C.Troncon[28], A.Tsirou[9], M-L.Turluer[39], I.A.Tyapkin[16], M.Tyndel[37], S.Tzamarias[22], B.Ueberschaer[52], O.Ullaland[9], V.Uvarov[42], G.Valenti[5], E.Vallazza[9], C.Vander Velde[2], G.W.Van Apeldoorn[31], P.Van Dam[31], J.Van Eldik[31], N.Vassilopoulos[35], G.Vegni[28], L.Ventura[36], W.Venus[37], F.Verbeure[2], M.Verlato[36], L.S.Vertogradov[16], D.Vilanova[39], P.Vincent[25], L.Vitale[46], E.Vlasov[42], A.S.Vodopyanov[16], V.Vrba[12], H.Wahlen[52], C.Walck[44], F.Waldner[46], M.Weierstall[52], P.Weilhammer[9], C.Weiser[17], A.M.Wetherell[9], D.Wicke[52], J.H.Wickens[2], M.Wielers[17], G.R.Wilkinson[35], W.S.C.Williams[35], M.Winter[10], M.Witek[18], K.Woschnagg[48], K.Yip[35], O.Yushchenko[42], F.Zach[25], A.Zaitsev[42], A.Zalewska[9], P.Zalewski[51], D.Zavrtanik[43], E.Zevgolatakos[11], N.I.Zimin[16], M.Zito[39], D.Zontar[43], G.C.Zucchelli[44], G.Zumerle[36]

[1] Ames Laboratory and Department of Physics, Iowa State University, Ames IA 50011, USA
[2] Physics Department, Univ. Instelling Antwerpen, Universiteitsplein 1, B-2610 Wilrijk, Belgium
and IIHE, ULB-VUB, Pleinlaan 2, B-1050 Brussels, Belgium
and Faculté des Sciences, Univ. de l'Etat Mons, Av. Maistriau 19, B-7000 Mons, Belgium
[3] Physics Laboratory, University of Athens, Solonos Str. 104, GR-10680 Athens, Greece
[4] Department of Physics, University of Bergen, Allégaten 55, N-5007 Bergen, Norway
[5] Dipartimento di Fisica, Università di Bologna and INFN, Via Irnerio 46, I-40126 Bologna, Italy
[6] Centro Brasileiro de Pesquisas Físicas, rua Xavier Sigaud 150, RJ-22290 Rio de Janeiro, Brazil
and Depto. de Física, Pont. Univ. Católica, C.P. 38071 RJ-22453 Rio de Janeiro, Brazil
and Inst. de Física, Univ. Estadual do Rio de Janeiro, rua São Francisco Xavier 524, Rio de Janeiro, Brazil
[7] Comenius University, Faculty of Mathematics and Physics, Mlynska Dolina, SK-84215 Bratislava, Slovakia
[8] Collège de France, Lab. de Physique Corpusculaire, IN2P3-CNRS, F-75231 Paris Cedex 05, France
[9] CERN, CH-1211 Geneva 23, Switzerland
[10] Centre de Recherche Nucléaire, IN2P3 - CNRS/ULP - BP20, F-67037 Strasbourg Cedex, France
[11] Institute of Nuclear Physics, N.C.S.R. Demokritos, P.O. Box 60228, GR-15310 Athens, Greece
[12] FZU, Inst. of Physics of the C.A.S. High Energy Physics Division, Na Slovance 2, 180 40, Praha 8, Czech Republic
[13] Dipartimento di Fisica, Università di Genova and INFN, Via Dodecaneso 33, I-16146 Genova, Italy
[14] Institut des Sciences Nucléaires, IN2P3-CNRS, Université de Grenoble 1, F-38026 Grenoble Cedex, France
[15] Research Institute for High Energy Physics, SEFT, P.O. Box 9, FIN-00014 Helsinki, Finland
[16] Joint Institute for Nuclear Research, Dubna, Head Post Office, P.O. Box 79, 101 000 Moscow, Russian Federation
[17] Institut für Experimentelle Kernphysik, Universität Karlsruhe, Postfach 6980, D-76128 Karlsruhe, Germany
[18] Institute of Nuclear Physics and University of Mining and Metalurgy, Ul. Kawiory 26a, PL-30055 Krakow, Poland
[19] Université de Paris-Sud, Lab. de l'Accélérateur Linéaire, IN2P3-CNRS, Bât. 200, F-91405 Orsay Cedex, France
[20] School of Physics and Chemistry, University of Lancaster, Lancaster LA1 4YB, UK
[21] LIP, IST, FCUL - Av. Elias Garcia, 14-1°, P-1000 Lisboa Codex, Portugal
[22] Department of Physics, University of Liverpool, P.O. Box 147, Liverpool L69 3BX, UK
[23] LPNHE, IN2P3-CNRS, Universités Paris VI et VII, Tour 33 (RdC), 4 place Jussieu, F-75252 Paris Cedex 05, France
[24] Department of Physics, University of Lund, Sölvegatan 14, S-22363 Lund, Sweden
[25] Université Claude Bernard de Lyon, IPNL, IN2P3-CNRS, F-69622 Villeurbanne Cedex, France
[26] Universidad Complutense, Avda. Complutense s/n, E-28040 Madrid, Spain
[27] Univ. d'Aix - Marseille II - CPP, IN2P3-CNRS, F-13288 Marseille Cedex 09, France
[28] Dipartimento di Fisica, Università di Milano and INFN, Via Celoria 16, I-20133 Milan, Italy
[29] Niels Bohr Institute, Blegdamsvej 17, DK-2100 Copenhagen 0, Denmark
[30] NC, Nuclear Centre of MFF, Charles University, Areal MFF, V Holesovickach 2, 180 00, Praha 8, Czech Republic
[31] NIKHEF-H, Postbus 41882, NL-1009 DB Amsterdam, The Netherlands
[32] National Technical University, Physics Department, Zografou Campus, GR-15773 Athens, Greece
[33] Physics Department, University of Oslo, Blindern, N-1000 Oslo 3, Norway
[34] Dpto. Fisica, Univ. Oviedo, C/P. Pérez Casas, S/N-33006 Oviedo, Spain
[35] Department of Physics, University of Oxford, Keble Road, Oxford OX1 3RH, UK
[36] Dipartimento di Fisica, Università di Padova and INFN, Via Marzolo 8, I-35131 Padua, Italy
[37] Rutherford Appleton Laboratory, Chilton, Didcot OX11 OQX, UK
[38] Dipartimento di Fisica, Università di Roma II and INFN, Tor Vergata, I-00173 Rome, Italy
[39] CEA, DAPNIA/Service de Physique des Particules, CE-Saclay, F-91191 Gif-sur-Yvette Cedex, France
[40] Istituto Superiore di Sanità, Ist. Naz. di Fisica Nucl. (INFN), Viale Regina Elena 299, I-00161 Rome, Italy
[41] Instituto de Fisica de Cantabria (CSIC-UC), Avda. los Castros, S/N-39006 Santander, Spain, (CICYT-AEN93-0832)
[42] Inst. for High Energy Physics, Serpukov P.O. Box 35, Protvino, (Moscow Region), Russian Federation
[43] J. Stefan Institute and Department of Physics, University of Ljubljana, Jamova 39, SI-61000 Ljubljana, Slovenia
[44] Fysikum, Stockholm University, Box 6730, S-113 85 Stockholm, Sweden
[45] Dipartimento di Fisica Sperimentale, Università di Torino and INFN, Via P. Giuria 1, I-10125 Turin, Italy
[46] Dipartimento di Fisica, Università di Trieste and INFN, Via A. Valerio 2, I-34127 Trieste, Italy
and Istituto di Fisica, Università di Udine, I-33100 Udine, Italy
[47] Univ. Federal do Rio de Janeiro, C.P. 68528 Cidade Univ., Ilha do Fundão BR-21945-970 Rio de Janeiro, Brazil
[48] Department of Radiation Sciences, University of Uppsala, P.O. Box 535, S-751 21 Uppsala, Sweden
[49] IFIC, Valencia-CSIC, and D.F.A.M.N., U. de Valencia, Avda. Dr. Moliner 50, E-46100 Burjassot (Valencia), Spain
[50] Institut für Hochenergiephysik, Österr. Akad. d. Wissensch., Nikolsdorfergasse 18, A-1050 Vienna, Austria
[51] Inst. Nuclear Studies and University of Warsaw, Ul. Hoza 69, PL-00681 Warsaw, Poland
[52] Fachbereich Physik, University of Wuppertal, Postfach 100 127, D-42097 Wuppertal, Germany
[53] On leave of absence from IHEP Serpukhov

1 Introduction

Supersymmetry (SUSY) [1] is a candidate theory to solve some of the puzzles which are present in the Standard Model (SM). In particular, SUSY gives a solution to the naturalness and hierarchy problems, which stem from the absence of any symmetry in the SM that can prevent the scalar sector from coupling to higher energy scales. Such a property of SUSY is present only if the mass splitting between ordinary particles and their supersymmetric partners is at most of the order of 1 TeV/c^2. Several arguments lead even to the conclusion that the lightest supersymmetric particles may have masses in the 100 GeV/c^2 region [2] and therefore be kinematically accessible at LEP.

Various SUSY models have been proposed. This paper presents a search for charginos in the framework of the Minimal Supersymmetric Standard Model (MSSM) [3] with R-parity conservation. This model has minimal additional particle content with respect to the SM (just one supersymmetric partner per particle plus one further complex Higgs doublet) and forbids single-particle production of supersymmetric particles.

Charginos are the mass eigenstates resulting from the mixing of the fermionic partners of W bosons (winos) and of charged Higgs bosons (charged higgsinos). There are two charginos, denoted by $\tilde{\chi}^{\pm}_{1,2}$, the lighter one being conventionally referred to by the lower index. They are expected to be among the lightest charged supersymmetric particles.

In e^+e^- collisions charginos are pair produced via Z/γ annihilation in the s-channel and through $\tilde{\nu}$ interchange in the t-channel. Apart from cases of strong destructive interference between these two processes, the chargino pair production cross-section at LEP energies is rather large, between several picobarns and a few tens of picobarns, depending on the mass and field composition of the chargino [4].

Chargino decays depend on the SUSY spectrum and therefore on the value of the SUSY parameters [4,5]. Assuming R-parity conservation, the most likely decays of the lightest chargino are to the lightest neutralino[†] and a pair of leptons or a pair of quarks. The former decay, i.e. $\tilde{\chi}^{\pm}_1 \to \tilde{\chi}^0_1\ \ell^{\pm}\ \nu$, can be mediated by a virtual W, a charged slepton, a sneutrino or charged Higgs bosons; the latter, $\tilde{\chi}^{\pm}_1 \to\ \tilde{\chi}^0_1\ q\ \bar{q}'$, by virtual W, squarks or charged higgses.

This paper concentrates on the case of the lightest chargino, referred to as $\tilde{\chi}^{\pm}$, decaying to the lightest neutralino, referred to as χ^0, via W^* exchange. The results, however, depend little on the exact branching ratios of the chargino or on the mediating process one considers, as will be shown.

Depending on whether both, one or none of the charginos decay leptonically, an event with two acoplanar leptons and missing energy (henceforth referred to as $\ell\ell$), an isolated lepton plus hadrons and missing energy ($jj\ell$) or a hadronic event with missing energy ($4j$) is expected. Such signatures are particularly clear; moreover, in the absence of W pair production, the background can be reduced essentially to zero. Since, in addition, the parameter space kinematically accessible can be experimentally explored with only minor restrictions, the chargino search in e^+e^- collisions above the Z peak is clearly a topic of major importance. Recent speculations [6] about the possibility that the R_b anomaly might be explained in terms of a light (close to the LEP I experimental limit) higgsino and/or scalar top quark contributions to the $Zb\bar{b}$ vertex add further interest to this search.

This paper describes a search for charginos carried out with the data taken by the DELPHI detector during the high energy run of LEP that took place in November 1995.

[†]Neutralinos are the mass eigenstates resulting from the mixing of photinos, zinos and neutral higgsinos. There are four of them, denoted, as for the charginos, by $\tilde{\chi}^0_{1,2,3,4}$ in order of increasing mass. The lightest one is expected to be the lightest supersymmetric particle and as such stable and behaving like a heavy neutrino.

During this LEP run DELPHI accumulated a total integrated luminosity of 2.91 pb^{-1} at $\sqrt{s}$ =130.4 GeV and of 3.01 pb^{-1} at $\sqrt{s}$ =136.3 GeV. Similar searches have been reported on by the other LEP experiments [7].

2 Detector description

DELPHI is a general purpose detector with a magnetic field of 1.2 Tesla provided by a large superconducting solenoid. The main tracking device is the cylindrical Time Projection Chamber (TPC), which extends over radial distances from 35 to 111 cm. Other cylindrical tracking devices used to reconstruct charged particle tracks at large angles with respect to the beam axis are the Vertex Detector, the Inner Detector and the Outer Detector. For particles emerging at smaller angles, the planar forward drift chambers (FCA and FCB) supplement the TPC for track reconstruction. The electromagnetic calorimetry in the forward region consists of the Forward Electromagnetic Calorimeter (FEMC), an array of lead glass blocks in the polar angular regions $10° < \theta < 36.5°$ and $143.5° < \theta < 170°$, and of the STIC, a sampling electromagnetic calorimeter, equipped also with two layers of scintillator counters, which covers the angular regions $1.66° < \theta < 10.6°$ and $169.4° < \theta < 178.34°$. As a barrel electromagnetic calorimeter, the High density Projection Chamber (HPC) covers the polar angle regions $43.1° < \theta < 88.7°$ and $91.3° < \theta < 136.9°$. The HPC is radially segmented into 9 layers and has a total of 144 modules. The hadron calorimeter (HCAL) is radially segmented into 4 layers and covers 98% of the solid angle. For muon detection, chambers are placed between the third and the fourth HCAL layer and outside the fourth layer, covering nearly all the solid angle.

The photon hermeticity of DELPHI in the regions not covered by the electromagnetic calorimeters is preserved using the information of dedicated taggers and of other detectors. The 40° taggers are photon counters, consisting of three scintillator layers behind 2 cm of lead each, used to detect photons otherwise missed in the regions at about 40° and 140° between the HPC and FEMC. Similar taggers have also been installed in the 90° polar region, which is not covered by the HPC. The Time of Flight detector (TOF), consisting of a single layer of 172 scintillation counters just outside the solenoid and covering the polar angular region $41° < \theta < 139°$, helps to increase the hermeticity in the regions in azimuthal angle between the modules of the HPC. The few azimuthal regions not covered by the TOF are equipped with another set of counters similar to the 40° taggers. Using LEP1 data it has been shown that the total photon detection efficiency of DELPHI is above 99% for photons of more than 5 GeV [8]. More details about the DELPHI detector can be found in [9].

3 Event Selection and Results

Before applying the channel-specific selection criteria, tracks not satisfying loose quality cuts on minimum and maximum momentum ($0.1 < p < 150$ GeV/c), on length ($l > 50$ cm) and on impact parameter (typically about 50 cm) with respect to the nominal beam interaction point were discarded, as well as neutral showers below a minimum energy of 100 MeV. "Good tracks" were then defined as those satisfying tighter requirements on the impact parameter (should typically be less than 5 cm in the $r\phi$ plane and less than 10 cm in z) and on the error on the momentum (less than 50%). These cuts varied slightly between channels.

3.1 Selection criteria for the $jj\ell$ channel

For the search for chargino candidates in the jet-jet-lepton topology ($jj\ell$), two different sets of selection criteria were used for the region where the difference of mass between the chargino and the lightest neutralino, ΔM, was high and the region where it was about 10 GeV/c^2 or lower. These regions will be referred to respectively as non-degenerate and degenerate case in the following.

In the non-degenerate case, the event was required to have at least three charged particles and a total (charged plus neutral) multiplicity of at least 10. Candidate events were then divided into two hemispheres defined by the thrust axis. The two vectors corresponding to the combined momenta in these hemispheres were required to have an acollinearity and acoplanarity of at least 10°. These cuts mainly reject background events of the type $e^+e^- \to q\,\bar{q}\,\gamma$, where the γ is emitted in the beam direction.

The presence of an isolated loosely identified electron or muon [9] of at least 3 GeV/c was then required. The LUND jet reconstruction algorithm was forced to reconstruct exactly two jets excluding the lepton candidate and the identified electron or muon was required to have an angle of at least 20° with respect to the axis of both jets. Events with an isolated lepton with a momentum higher than 25 GeV/c were rejected.

The missing transverse momentum of the event was required to be larger than 5 GeV/c and the polar angle of the missing momentum had to be outside the forward and backward regions at 20° with respect to the beam axis. Furthermore, at most 50% of the visible energy had to be in the same regions. These cuts mainly reject events coming from two-photon processes.

Events passing the above cuts were finally required to have a visible mass smaller than 65 GeV/c^2 and a hadronic mass smaller than 45 GeV/c^2. This further reduces the $q\,\bar{q}\,\gamma$ background.

For the degenerate case, some changes were made to the selection criteria of the $jj\ell$ topology in order to increase the selection efficiency. The lower bound on the total multiplicity was removed; the cut on the minimum momentum of the isolated lepton was relaxed down to 1 GeV/c and that on the minimum missing transverse momentum to 2 GeV/c. In order to compensate for the loss of purity due to these looser criteria, the cuts in visible mass and in the percentage of energy in the 20° forward and backward cones were lowered to 20 GeV/c^2 and 20%, respectively.

3.2 Selection criteria for the $4j$ channel

Events in the hadronic topology ($4j$) were selected with the following criteria. As in the preceding topology, charged and total multiplicities of at least 3 and 10, respectively, were required and the number of reconstructed jets was forced to two. An acollinearity and acoplanarity higher than 30° were imposed in order to reject $e^+e^- \to q\,\bar{q}\,\gamma$ events, where the γ was emitted in the beam direction.

The absence of an isolated lepton, according to the above definition, was also demanded. As before, the missing transverse momentum of the event was required to be larger than 5 GeV/c and the energy in the forward and backward 20° cone had to be at most 50% of the visible energy. The polar angle of the missing momentum was required in this case to be in the region $30° < \theta_{\not p} < 150°$. These cuts were devised to reject mainly events from $\gamma\,\gamma$ processes.

Events with a cluster of neutral electromagnetic energy with more than 10 GeV in any of the electromagnetic calorimeters were also rejected[‡]. This cut was intended to

[‡]Hits in the STIC were attributed to neutral particles.

reject events with an energetic initial state radiation. Finally, a visible mass smaller than 55 GeV/c^2 was demanded.

No looser cuts were used in this case for the degenerate region, since there the background is not so strongly suppressed as for the $jj\ell$ channel, due to the absence of the isolated lepton signature.

3.3 Selection criteria for the $\ell\ell$ channel

Events in the leptonic topology ($\ell\ell$) were selected with the following purely topological cuts, which were devised to yield good efficiency and purity both in the non-degenerate and in the degenerate regions, including $\chi^+\chi^-$ events with more than just two charged particles (e.g. leptonic events with at least one 3-prong τ decay or low multiplicity semileptonic events which might have been rejected by the $jj\ell$ cuts defined in 3.1).

The events had to contain at least two charged particles associated to good tracks, the total multiplicity being smaller than eight. The two most energetic particles had to be both in the polar angular region $20^\circ < \theta < 160^\circ$, isolated from each other by at least 5° in the polar angle and with an acoplanarity between them larger than 10°.

The missing momentum had to be in the polar angular region $20^\circ < \theta_{\not p} < 160^\circ$ and the visible energy had to be smaller than 50 GeV. Events with isolated neutral electromagnetic clusters of more than 20 GeV and events with isolated signals in the hermeticity taggers were rejected to avoid background events from radiative return to the Z^0 . Finally, the kinematic quantities in the transverse plane were used to reject the two-photon background. The missing transverse momentum was demanded to be greater than 2.5 GeV/c and the squared momentum $\tilde{p}_t^2 = \frac{p_1^2 p_2^2 sin^2\delta}{p_1^2+p_2^2-2|p_1||p_2|cos\delta}$ perpendicular to the projection of the thrust onto the transverse plane was demanded to be greater than 0.3 GeV^2/c^2 in order to suppress $\gamma\gamma \to \tau^+\tau^-$ events in which the two most energetic particles were the result of 1-prong decays of the τ's. The variables p_1 and p_2 were the components of the momenta of the two most energetic particles in the transverse plane and δ the difference of their azimuthal angles).

Additional tighter cuts were used in the cases of a missing transverse momentum close to the cut or of a charged multiplicity larger than two. In the first case (2.5 GeV/c $< \not p_t <$ $0.025\sqrt{s}$/c) the acoplanarity had to be larger than 20°, the momentum of the second most energetic particle to be larger than 0.5 GeV/c and less than 20% of the visible energy had to be in the 30° forward cone. In the second case the acoplanarity had to be greater than 20° and smaller than 170°, the visible mass larger than 4 GeV/c^2 and the missing transverse momentum larger than $0.025\sqrt{s}$/c.

3.4 Efficiencies

The efficiencies of the above selection criteria were estimated using simulated chargino events generated with the program SUSYGEN [10] at the two beam energies and processed through the full DELPHI simulation and reconstruction programs [9]. In total fifteen mass combinations were chosen in two ranges of chargino masses ($M_{\chi_1^\pm} \approx 64$ GeV/c^2 and $M_{\chi_1^\pm} \approx 55$ GeV/c^2), considering also cases in which the second lightest neutralino or the sneutrino are lighter than the lightest chargino.

Fig.1 shows the detection efficiencies for the three modes, considering for each mode all sets of cuts. They are the same at the two energies, within the statistical uncertainty. The contribution of the $4j$ and $\ell\ell$ selections to the $jj\ell$ detection efficiency is not negligible: in some $jj\ell$ events the lepton is either not isolated, due to the isotropic chargino decay, or

not identified; hence the event migrates to the $4j$ topology. In other cases, especially when ΔM is small, the $jj\ell$ events have a small charged multiplicity and a soft not identified lepton; so they migrate to the leptonic topology.

The chargino detection efficiency for the $jj\ell$ mode is typically 70-80%. It decreases drastically in the degenerate region, essentially due to the cut in missing transverse momentum. This efficiency is given relative to the number of $jj\ell$ chargino events with one electron or muon, including those coming from τ leptonic decays.

For the $4j$ mode, the selection efficiency depends more strongly both on the chargino mass and on the chargino–neutralino mass difference even in the non-degenerate region, showing well separated curves for different masses. The maximum efficiency is reached for a ΔM of 15-20 GeV/c^2 and decreases at higher mass differences, essentially due to the cut on the visible mass, and at lower ΔM, due to the cut on $\not{p}_t$.

The average chargino detection efficiency for the $\ell\ell$ mode for $\Delta M > 15$ GeV/c^2 is 50% and again decreases with the chargino–neutralino mass difference. It has been checked that, when the sneutrino is lighter than the chargino, a similar dependence of the efficiency for the $\ell\ell$ mode on ΔM is obtained, taking in this case ΔM as the chargino–sneutrino mass difference.

Assuming that the chargino has the same branching ratios as the W, the overall detection efficiencies shown in Fig. 1.d are obtained.

3.5 Background estimation

An estimation of the most important background processes used simulated events with at least an order of magnitude more statistics than the number expected for the real accumulated luminosities. For the hadronic $\gamma\,\gamma$ processes, five times higher statistics than those expected in the data were obtained after applying a filter at the generation level to reject events kinematically well outside the angular cuts used in the analysis. The programs PYTHIA and TWOGAM [11] were used and the events generated at the two beam energies were processed through the full chain of simulation and reconstruction programs [9]. The backgrounds considered were $e^+e^- \rightarrow f\,\bar{f}\,\gamma$, where the dominant contribution comes from radiative return events, the $\gamma\gamma$ processes (VDM, QPM and QCD components [2]) and some less important processes in terms of cross-section, such as $e^+e^- \rightarrow W\,W^*$, $e^+e^- \rightarrow Z\,Z^*$, $e^+e^- \rightarrow W\ e\ \nu$ and $e^+e^- \rightarrow Z\ e\ e$, where Z is always to be understood as a mixing of Z and γ^*. The program EXCALIBUR [12] was used to cross-check the total background level from four-fermion $e^+e^- \rightarrow l^+l^-\nu\bar{\nu}$ processes.

The expected background after cuts, combining the two energy samples, is 0.65 events for the $\ell\ell$ topology, 0.1 events for the $jj\ell$ topology and 0.2 events for the $4j$ topology.

3.6 Candidates

No events were selected in the data in the $jj\ell$ and $4j$ topologies while two events remained after cuts in the $\ell\ell$ topology.

One event has two charged particles, one in the barrel region identified as a muon, the other identified as an electron in the forward electromagnetic calorimeter. The only additional sign of activity in the event is a small energy deposit in the STIC. The azimuthal coordinate of this deposit is however almost coincident with the azimuthal direction of the missing momentum and the hit pattern compatible with that expected for a muon. The extremely low probability of such a pattern being due to the beam, tested on random events, allowed this event to be rejected without inducing any appre-

ciable signal inefficiency. Events of this kind were found in the simulation of the process $e^+e^- \to \gamma^* e^+e^- \to l^+l^- e^+e^-$, with a rate of 0.07 events expected for the accumulated luminosity. An alternative hypothesis also in terms of standard physics is that of a single–tag $\gamma\gamma \to l^+l^-$ event, with a minimum ionizing particle entering the STIC. From a kinematic evaluation at the generation level about 0.06 such events are expected.

The second event also has two particles, as can be seen in Fig. 2. One is an electron well identified in the HPC. The other one is seen by the veto taggers at 40°, produces some activity in the FCB chambers and leaves a small energy deposit in the hadron calorimeter; hence it is well compatible with being an electron.

The very high (170°) acoplanarity angle and the high missing transverse momentum (15.3 GeV/c) allows the two-photon hypothesis to be excluded. The most convincing explanation in terms of standard physics is a 4-fermion $\nu\bar{\nu}l^+l^-$ event, a process which is expected to contribute 0.2 events to the total background.

This event, registered at $\sqrt{s}$= 130.4 GeV, has been taken into account in the calculation of the exclusion limits for the non-degenerate case, giving conservatively an upper limit on the number of candidates above background of 4.24 at 95% confidence level for mass limits below 65.2 GeV/c^2 and of 3.0 for mass limits above that value. On the contrary it has not been considered in the limits for the degenerate case, since the collinearity, the visible energy (19.4 GeV) and the missing transverse momentum are too high for such a scenario. Hence the corresponding upper limit was 3.0 candidates at the 95% confidence level.

4 Limits

In the MSSM [3] the production of charginos depends, at a given energy, only on M_2, the low-energy scale mass parameter of the wino (the fermionic partner of the standard model SU(2) triplet) on μ, the low-energy scale parameter of the Higgs terms in the supersymmetric lagrangian, on $\tan\beta$, the ratio between the vacuum expectation values of the Higgs doublets, and on the sneutrino mass. When the sneutrino is heavy or the chargino is higgsino-like ($M_2 \gg |\mu|$), the production cross-section is generally well above 1 pb. On the contrary, when the sneutrino is light and the chargino is mostly a wino ($|\mu| \gg M_2$), the s-channel production via Z/γ annihilation and the t-channel production via $\tilde{\nu}$ exchange interfere destructively, so that the production cross-section may be strongly reduced.

In chargino decays, the mass parameter M_1 of the bino (the fermionic partner of the standard model U(1) singlet) is also relevant, since it determines the neutralino masses. However, assuming unification of the gaugino mass parameters at the GUT scale [13], the relation $M_1 \approx 0.5 M_2$ holds. Hence M_2 can be considered the only free gaugino mass parameter and will be called M in the following. A higgsino-like chargino couples weakly to squarks and sleptons [5], so that the chargino decay mainly proceeds through virtual W. On the contrary, a wino-like chargino couples preferentially to squarks and sleptons, when they become sufficiently light. If for example the $\tilde{\nu}$ or the $\tilde{\ell}$ are lighter than a wino-like chargino, the decay modes $\tilde{\chi}^\pm \to \ell\,\tilde{\nu}$ or $\tilde{\chi}^\pm \to \tilde{\ell}\,\nu$ become dominant, producing totally different branching ratios to the three considered topologies, compared to the decay through a virtual W.

In the calculation of the lower limits[§] on the chargino mass, it is assumed that the sneutrino and squark masses are large (1 TeV) and that the decay $\tilde{\chi}^\pm \to \tilde{\chi}^0 W^*$ is dom-

[§] All limits and exclusion regions in this section are given at the 95% confidence level.

inant. The lower limit[¶] for the chargino mass, obtained combining all three topologies, is 66.8 GeV/c^2 in the non-degenerate case and 63.8 GeV/c^2 in the most degenerate case which has been considered (ΔM = 5 GeV/c^2). No limits are set for $\Delta M < 5$ GeV/c^2. The corresponding upper limits for the cross-section at $\sqrt{s}$= 136.3 GeV are 1.64 pb and 3.35 pb, respectively.

Given that all topologies are detected with high efficiency, changes in the branching ratios of the chargino would not significantly affect the above limits on masses and cross-sections [8], as long as the sleptons and squarks are heavier than the chargino or the relevant mass differences are larger than 10 GeV/c^2. A light sneutrino or charged slepton would enhance the purely leptonic channel, whereas a light stop would enhance the purely hadronic channel. The worst case is when the sneutrino or a charged slepton are lighter than the chargino, which hence always decays leptonically: then the lower limit on the chargino mass is 64.9 GeV/c^2 and the maximum cross-section 2.8 pb, provided $m_{\tilde{\chi}^\pm} - m_{\tilde{\nu}} > 10$ GeV/c^2 or $m_{\tilde{\chi}^\pm} - m_{\tilde{l}^\pm} > 10$ GeV/c^2.

As to the impact of the sneutrino mass on the chargino production cross-sections and on the mass limits, Fig. 3 and Fig. 4 show the scatter plots of the possible chargino production cross-sections that can be obtained in the MSSM as a function of the chargino mass when the sneutrino mass is in the range 41 GeV/c^2 $< m_{\tilde{\nu}} <$ 100 GeV/c^2 and when it is 1 TeV/c^2. The parameters M and μ have been varied between 0 GeV/c^2 $< M <$ 800 GeV/c^2 and –400 GeV/c^2 $< \mu <$ 400 GeV/c^2, and $\tan\beta$ has been set to three different values, namely 1, 1.5 and 35.

Fig. 3 corresponds to the non-degenerate case and Fig. 4 to the highly degenerate case (ΔM = 5 GeV/c^2). In this latter instance the influence of the sneutrino mass is negligible, since a low chargino–neutralino mass differences requires the chargino to be mostly higgsino and therefore to couple very weakly to the sneutrino.

For a heavy sneutrino, non-degenerate chargino production can be excluded essentially up to the kinematic limit, namely 66.8 GeV/c^2, as can be deduced from Fig. 3. For the hypothesis of a light sneutrino (41 GeV/c^2 $< m_{\tilde{\nu}} <$ 100 GeV/c^2) and the smallest cross-section, a lower limit of 56.3 GeV/c^2 can be placed on the chargino mass in the non-degenerate case. On the other hand, for the highly degenerate case the chargino mass limit remains essentially at 63.8 GeV/c^2, with no dependence on the sneutrino mass. The corresponding upper limits on the cross-section at 136.3 GeV are 1.15 pb for the non-degenerate case and 3.35 pb for the highly degenerate one.

These mass and cross-section limits are summarized in Table 1.

In Fig. 5 is shown the region in the chargino–neutralino mass plane excluded for $\tan\beta$ = 1, 1.5 and 35.

In Fig. 6 are shown the regions in the (M , μ) plane that can be excluded for values of $\tan\beta$ = 1.0 (Fig. 6.a), $\tan\beta$ = 1.5 (Fig. 6.b) and $\tan\beta$ = 35 (Fig. 6.c).

5 Summary

A search for the lightest chargino at $\sqrt{s}$ = 130.4 and 136.3 GeV has been carried out with the DELPHI detector. One event remains, after cuts, in the two acoplanar leptons plus missing energy mode, to be compared with the total expected background of 0.95 events.

[¶]First only the luminosity at 136.3 GeV was used for each scenario in the calculation of the limits on the chargino mass; if the resulting mass limit was accessible at 130.4 GeV, it was recalculated using the luminosities at both energies and taking into account the different dependence of the cross-section on the chargino mass.

Scenario	Light sneutrino		Heavy sneutrino		Efficiency
	$M_{\chi^\pm}^{min}$	σ^{max}	$M_{\chi^\pm}^{min}$	σ^{max}	
$\Delta M > 10$ GeV/c^2	56.3 GeV/c^2	1.15 pb	66.8 GeV/c^2	1.64 pb	60.9%
$\Delta M = 5$ GeV/c^2	63.8 GeV/c^2	3.35 pb	63.8 GeV/c^2	3.35 pb	17.4%

Table 1: 95% confidence level limits for the chargino mass and the cross-section at 136.3 GeV for the non-degenerate and a highly degenerate scenario. The cases of a light (41 GeV/c^2 $< m_{\tilde{\nu}} <$ 100 GeV/c^2) or a heavy ($m_{\tilde{\nu}} = 1$ TeV/c^2) sneutrino are considered.

The 95% confidence level lower limits that can be imposed on the lightest chargino mass are $m_{\tilde{\chi}_1^\pm} > 66.8$ GeV/c^2 for the non-degenerate scenario ($\Delta M > 10$ GeV/c^2) and $m_{\tilde{\chi}_1^\pm} > 63.8$ GeV/c^2 for the highly degenerate scenario ΔM=5 GeV/c^2, if the sneutrino mass is $m_{\tilde{\nu}} = 1$ TeV/c^2. No mass limits were deduced for higher degeneracies.

If the sneutrino mass is in the range 41 GeV/c^2 $< m_{\tilde{\nu}} <$ 100 GeV/c^2, the corresponding mass limits are $m_{\tilde{\chi}_1^\pm} > 56.3$ GeV/c^2 for the non-degenerate scenario and $m_{\tilde{\chi}_1^\pm} >$ 63.8 GeV/c^2 for the highly degenerate scenario.

The 95% confidence level upper limits that can be set on the chargino production cross-section at $\sqrt{s} = 136.3$ GeV, assuming a non-degenerate scenario, are 1.64 pb for a heavy sneutrino and 1.15 pb for a light sneutrino.

For a chargino–neutralino mass difference of 5 GeV/c^2, the cross-section upper limit is 3.35 pb independently of the sneutrino mass.

Acknowledgements

We are greatly indebted to our technical collaborators and to the funding agencies for their support in building and operating the DELPHI detector. We are particularly thankful to the members of the CERN-SL Division for the excellent performance of LEP during the high energy run of 1995.

References

[1] Y.A. Golfand and E.P. Likhtman, JETP Lett. **13** (1971) 323;
D.V. Volkhov and V.P. Akulov, Phys. Lett. **B46** (1973) 109;
J. Wess and B. Zumino, Nucl. Phys. **B70** (1974) 39.

[2] R. Barbieri and G.F. Giudice, Nucl. Phys. **B306** (1988) 63;
S. Dimopoulos and G.F. Giudice, Phys. Lett. **B357** (1995) 573.

[3] See for instance the classical reviews:
P. Fayet and S. Ferrara, Phys. Rep. **32** (1977) 249;
H.P. Nilles, Phys. Rep. **110** (1984) 1;
H.E. Haber and G.L. Kane, Phys. Rep. **117** (1985) 75;
R. Barbieri, Riv. Nuovo Cim. **11** (1988) 1.

[4] A. Bartl, H. Fraas and W. Majerotto, Z. Phys. **C30** (1986) 441;
A. Bartl, H. Fraas and W. Majerotto, Z. Phys. **C41** (1988) 475;
A. Bartl, H. Fraas, W. Majerotto and B. Mösslacher, Z. Phys. **C55** (1992) 257.

[5] J.L. Feng and M.J. Strassler, Phys. Rev. **D51** (1995) 4661.

[6] G. Altarelli, R. Barbieri and F. Caravaglios, Phys. Lett. **B314** (1993) 357;
J.D. Wells, Ch. Kolda and G.L. Kane, Phys. Lett. **B338** (1994) 219;
G.L. Kane, R.G. Stuart and J.D. Wells, Phys. Lett. **B354** (1995) 350;
P. Chankowski and S. Pokorski, Phys. Lett. **B366** (1996) 188.

[7] ALEPH Collaboration, D. Buskulic et al., "Search for supersymmetric particles in e+e- collisions of centre-of-mass energies of 130 and 136 GeV", CERN PPE/96-010;
L3 Collaboration, M. Acciarri et al., "Search for Supersymmetric Particles at 130 GeV $< \sqrt{s} <$ 140 GeV at LEP", CERN PPE/96-029;
OPAL Collaboration, G. Alexander et al., "Search for Chargino and Neutralino Production Using the OPAL Detector at $\sqrt{s}$= 130-136 GeV at LEP", CERN PPE/96-020.

[8] P. Rebecchi, "Optimisation de l'herméticité du détecteur DELPHI pour la recherche de particules supersymétriques à LEP2", Thesis, LAL 96-30.

[9] DELPHI Collaboration, P. Aarnio et al., Nucl. Instr. Meth. **A303** (1991) 233;
DELPHI Collaboration, P. Abreu et al., CERN PPE 95-194, to appear in Nucl. Instr. Meth.

[10] S. Katsanevas and S. Melachroinos, SUSYGEN, in "*Physics at LEP2*", CERN 96-01 (Vol. 2) 328.

[11] T. Sjöstrand, PYTHIA 5.7 AND JETSET 7.4, Physics and Manual, Comp. Phys. Comm. **82** (1994) 74;
S. Nova, A. Olshevski and T. Todorov, TWOGAM, "*A Monte Carlo event generator for two-photon physics* ", DELPHI note 90-35 PROG 152.

[12] F.A. Berends, R. Kleiss and R. Pittau, EXCALIBUR, Comp. Phys. Comm. **85** (1995) 437.

[13] G.F. Giudice et al., in "*Physics at LEP2*", CERN 96-01 (Vol. 1) 349 and references therein.

[14] OPAL Collaboration, G. Alexander et al., "Topological Search for the Production of Neutralinos and Scalar Particles", CERN PPE/96-019.

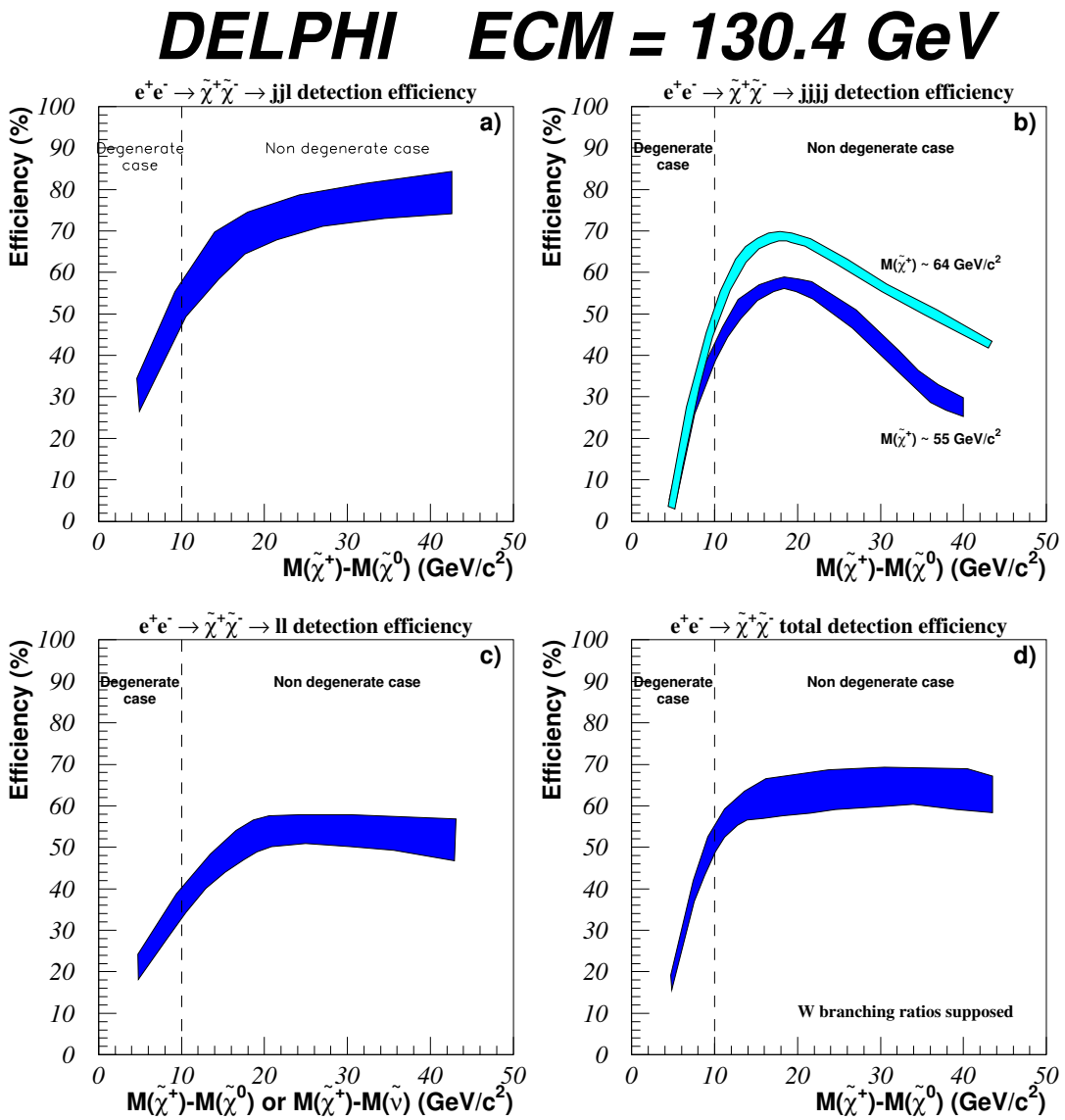

Figure 1: Chargino detection efficiency for the three modes: a) $jj\ell$, b) $4j$ and c) $\ell\ell$, obtained summing over the three selection criteria. d) Overall chargino detection efficiency obtained summing over the three selection criteria and assuming for the chargino decay branching ratios equal to those of the W. The bands correspond to the statistical error combined with the effect of generating points at different chargino masses.

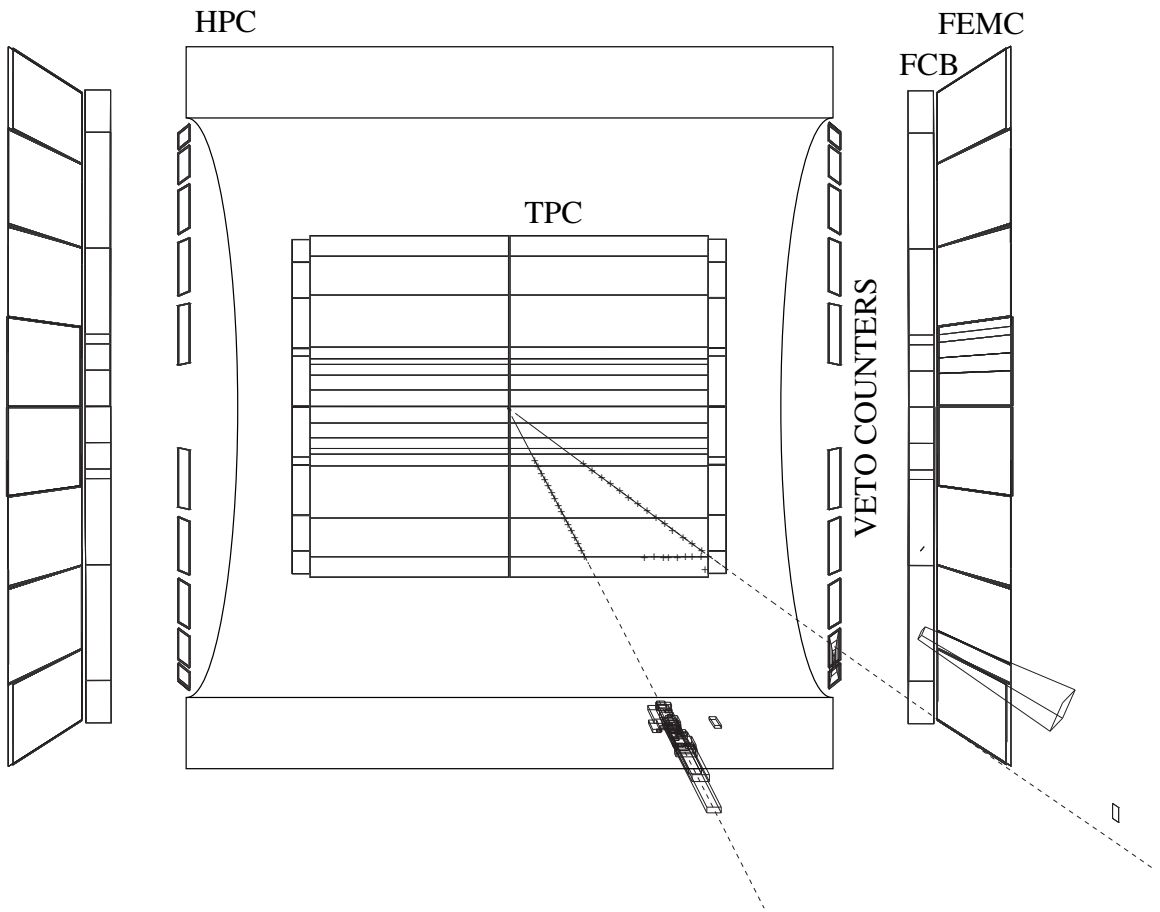

Figure 2: Representation of the event remaining in the data after cuts. The TPC, the two crowns of the 40° taggers, the FCB chambers and the FEMC calorimeter are shown. The high energy deposit of the 11.7 GeV/c particle in the barrel electromagnetic calorimeter, together with the signal of the 7.7 GeV/c particle in the 40° taggers, its small energy deposit in the hadronic calorimeter and its effect in the FCB are visible.

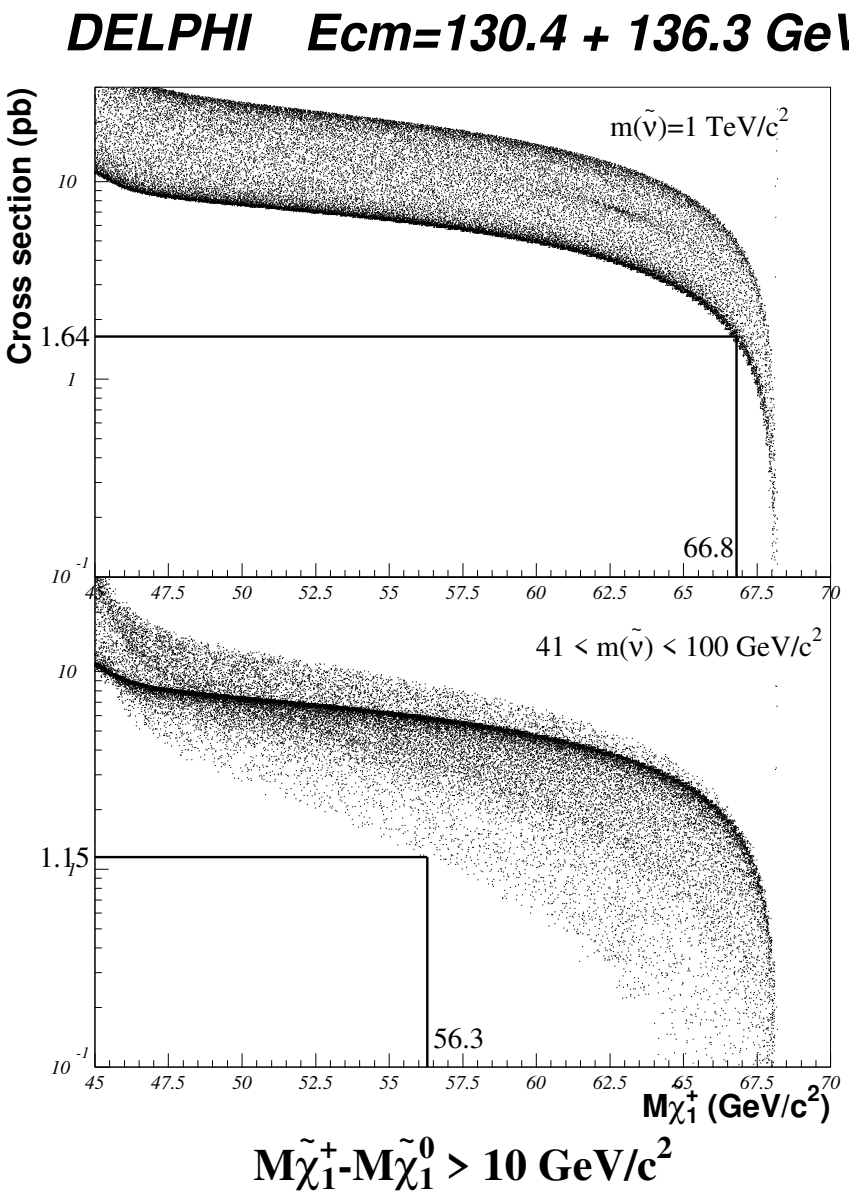

Figure 3: Scatter plot of the expected cross-section at 136.3 GeV versus the chargino mass in the non-degenerate scenario ($\Delta M > 10$ GeV/c^2). The MSSM parameters M and μ have been varied in the ranges $0 < M < 800$ GeV/c^2 and –400 GeV/c^2 $< \mu <$ 400 GeV/c^2 for three different values of $\tan\beta$: 1, 1.5 and 35. A very heavy sneutrino ($m_{\tilde{\nu}}$= 1 TeV/c^2) has been assumed in the upper part and a light sneutrino (41 GeV/c^2 $< m_{\tilde{\nu}} <$ 100 GeV/c^2) in the lower one.

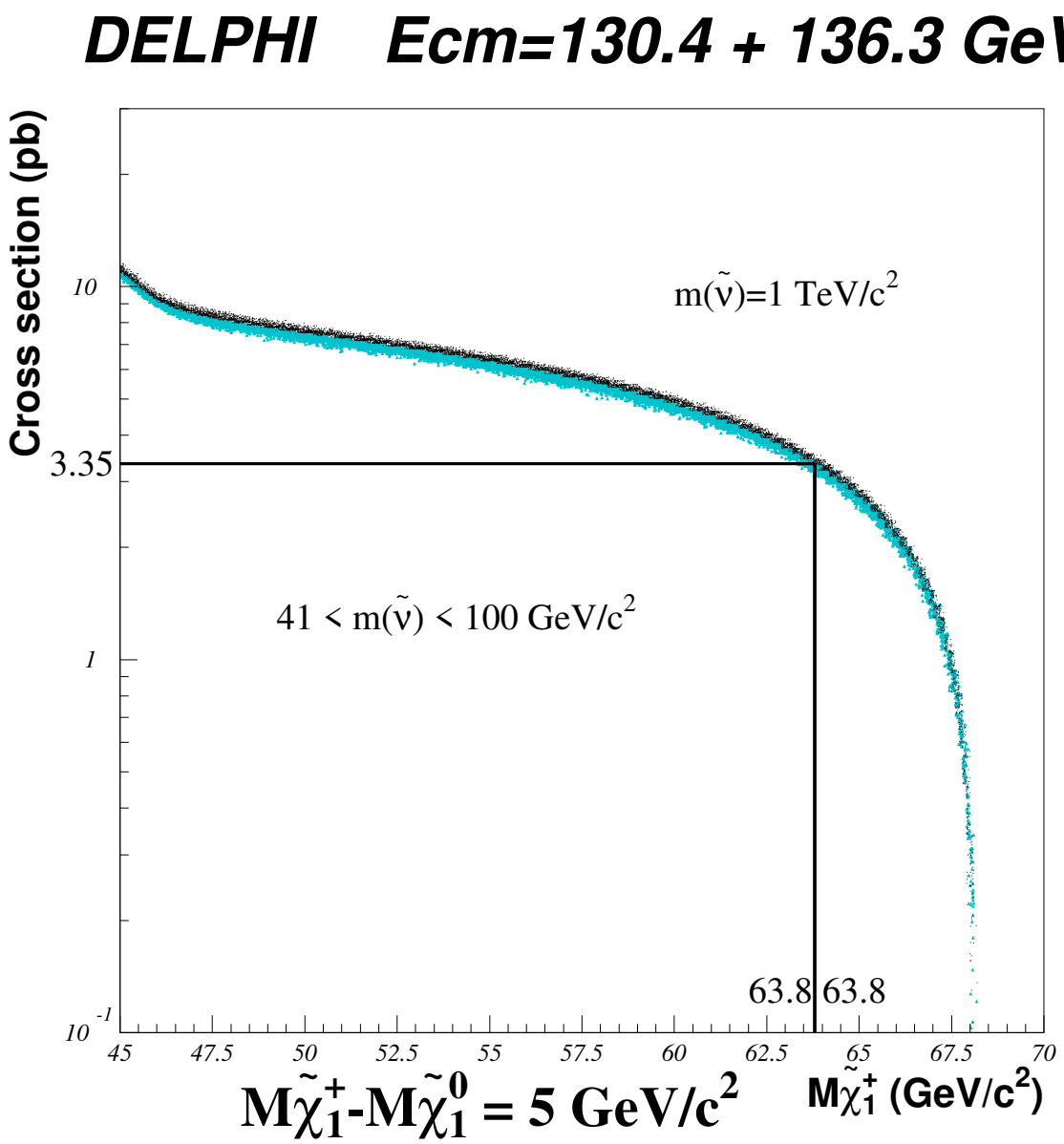

Figure 4: Scatter plot of the expected cross-section at 136.3 GeV versus the chargino mass in the highly degenerate scenario (ΔM = 5 GeV/c^2). The MSSM parameters M and μ have been varied in the same ranges as for Fig. 3. The two bands correspond to different assumptions on the sneutrino mass, a light sneutrino (41 GeV/c^2 < $m_{\tilde{\nu}}$< 100 GeV/c^2) for the thick grey dots and a very heavy sneutrino ($m_{\tilde{\nu}}$= 1 TeV/c^2) for the thin black ones. The corresponding limits on the chargino mass and cross-section are shown.

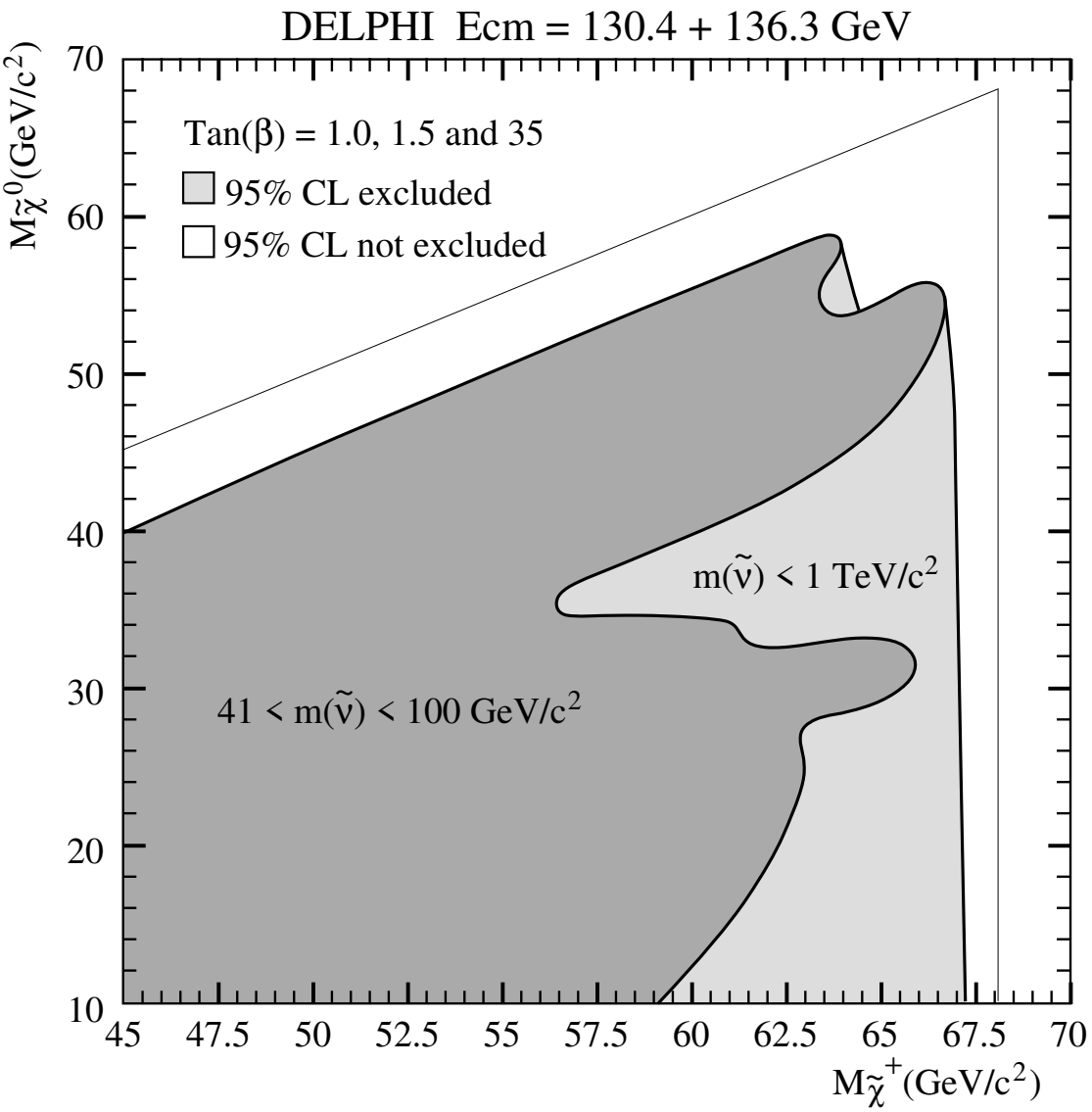

Figure 5: Regions excluded at the 95% C.L. in the ($m_{\tilde{\chi}_1^\pm}$, $m_{\tilde{\chi}_1^0}$) plane. Three different values of $tan\,\beta$ have been used: 1, 1.5 and 35. The regions excluded when the sneutrino is light (41 GeV/c^2 $< m_{\tilde{\nu}} <$ 100 GeV/c^2) are shown in dark grey; the additional regions excluded when the sneutrino is very heavy ($m_{\tilde{\nu}} = 1$ TeV/c^2) are shown in light grey. The outermost line corresponds to the kinematic limit.

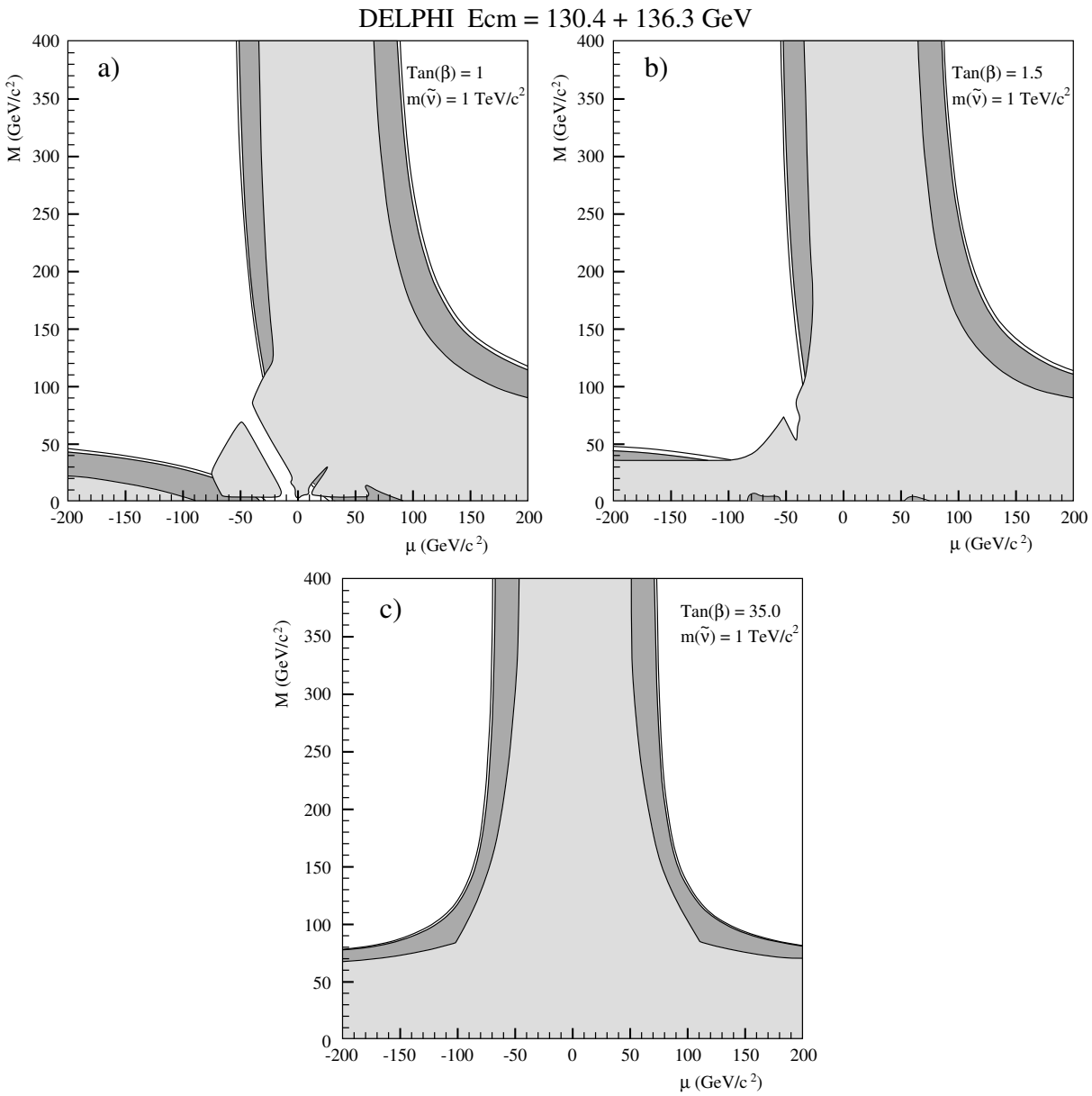

Figure 6: Regions excluded at the 95% C.L. in the (M , μ) plane are shown in dark grey for a) $\tan\beta = 1.0$, b) $\tan\beta = 1.5$ and c) $\tan\beta = 35$. The regions in light grey inside the curve had already been excluded at LEP1 by chargino or by neutralino searches [14]. The outermost line corresponds to the kinematic limit.